Pis'ma v ZhETF, vol. 97, iss. 8, pp. 529 – 535 © 2013 April 25

Non-stationary regimes of surface gravity wave turbulence

R. Bedard, S. Lukaschuk[1)], *S. Nazarenko*[+]

Department of Engineering, University of Hull, Hull, HU6 7RX, UK

[+]*Mathematics Institute, University of Warwick, Coventry, CV4 7AL, UK*

Submitted 26 February 2013

Resubmitted 27 March 2013

We present experimental results about rising and decaying gravity wave turbulence in a large laboratory flume. We consider the time evolution of the wave energy spectral components in ω- and k-domains and demonstrate that emerging wave turbulence can be characterized by two time scales – a short dynamical scale due to nonlinear wave interactions and a longer kinetic time scale characterising formation of a stationary wave energy spectrum. In the decay regime we observed the maximum of the wave energy spectrum decreasing in time initially as the power law, $\propto t^{-1/2}$, as predicted by the weak turbulence theory, and then exponentially due to viscous friction.

DOI: 10.7868/S0370274X13080055

Surface gravity waves generated by wind represent a practically important and most studied example of wave turbulence. Such waves are of small amplitude in most natural cases and can be described by a weak turbulence theory (WTT) [1]. A small parameter is the ratio of the wave height to its length $\eta/\lambda \ll 1$ or the wave steepness $k\eta$, where $k = 2\pi/\lambda$ is the wave vector. The WTT considers statistics of isotropic ensembles of dispersive weakly nonlinear interactive waves and predicts a scale invariant form of the wave energy spectra $E_k \propto k^{-\mu}$ and $E_\omega \propto \omega^{-\nu}$ within the universal interval (k_f, k_d). Here ω is the wave frequency, the subscripts f and d are related to the forcing and dissipative scales respectively. It is assumed that $k_d \gg k_f$. For isotropic surface gravity wave turbulence the WTT predictions for the spectral exponents are $\mu = 7/2$, $\nu = 4$ known as Kolmogorov–Zakharov (K–Z) spectrum.

K–Z spectrum was confirmed numerically in [2], though within less than a decade universal interval. The most advanced field experiments done by Hwang et al. [3] show the energy spectra exponents close to the WTT predictions, though the wave fields in that experiment were not isotropic and near surface wind was not measured. Incomplete knowledge of external factors such as wind, currents and various gradients of physical parameters makes interpretations of the field experiments difficult. Parameters of laboratory experiments are under much better control and some small scale experiments with capillary wave turbulence demonstrate good agreement of measured ν-exponents with the WTT predictions, see for example [4]. In our recent experiments with gravity waves in a large flume [5, 6] we observed dependence of the ν- and μ-exponents from the averaged wave amplitude or the coefficient of wave nonlinearity $\gamma = k_f\sqrt{\langle\eta^2(t,r)\rangle}$, where $\langle ...\rangle$ denotes mean taken over the time or space. We explained this dependence as a result of three possible mechanisms [7]: four-wave interactions, finite size effects and wave breaking. Our measured exponents asymptotically approach the values predicted by the WTT at large wave amplitudes with $\gamma \approx 0.25$, where apparently that theory should not be applied.

Most of the previous laboratory studies of wave turbulence were concerned with statistics of stationary regimes. Just a few experiments dealt with non-stationary cases and all of them are about the decay of capillary wave turbulence [8, 9]. As far as we are aware, characteristics of non-stationary gravity wave turbulence had never been studied experimentally. This paper presents our new experimental observations of rising and decaying regimes of gravity wave turbulence and their analysis in terms of temporal evolutions of the energy spectral modes in ω- and k-domains. For the first time we present here the measured characteristic time for wave turbulence formation and observations of a non-monotonic character of the spectral mode decay at the intermediate scales within the universal interval.

There are two time scales which will be useful for our further discussion. The dynamical scale τ_D is the characteristic time of deterministic nonlinear dynamical equations for surface gravity waves. It can be derived from a knowledge that the leading order wave interac-

[1)]e-mail: S.Lukaschuk@hull.ac.uk

tion process for surface gravity waves is four-wave and therefore $\dot{\eta_1} \propto \eta_2\eta_3\eta_4$. It follows from here that the dynamical time is inversely proportional to the square of the wave amplitude. The rest of the expression can be reconstructed from dimensionality by adding the wave frequency ω and the gravity constant g:

$$\tau_D \sim \frac{g^2}{\omega^5\eta^2}. \tag{1}$$

The kinetic time scale can be obtained from the dimensional analysis of the kinetic equation [1] based on the fact that, the inverse characteristic time must be proportional to the fourth power of the wave amplitude and the rest is reconstructed dimensionally:

$$\tau_K \sim \frac{g^4}{\omega^9\eta^4} = \tau_D^2\omega = \gamma^{-2}\,\tau_D. \tag{2}$$

For our typical experiment $\eta \sim 5\,\text{cm}$, $\omega \sim \omega_f = 2\pi f$, where f is the forcing frequency which is about 1 Hz. We have the nonlinearity parameter $\gamma \sim 0.2$, $\tau_D \sim 4\,\text{s}$ and $\tau_K \sim 100\,\text{s}$. Note that the timescales are very sensitive to the values of η and ω_f. Once the forcing is switched off the kinetic time rapidly increases due to the strong dependence of τ_K on η.

Let us suppose that the kinetic equation of weak wave turbulence is valid from the very first moment after the pumping of energy is turned on, and consider formation of the steady state spectrum. There are several types of self-similar evolution. To identify one for gravity waves we notice that this is a finite capacity system, i.e. only a finite amount of wave energy is necessary to fill up the high-frequency tail of the K–Z-spectrum for whatever large inertial intervals. Thus, no matter how high the dissipation frequency is, the propagating front of the spectrum will reach from the forcing to the dissipation frequency in a finite time which is of an order of the kinetic characteristic time τ_k (2). It is interesting that the spectrum left behind a propagating front is steeper than the K–Z-spectrum. The K–Z-spectrum will finally form as a reflection wave propagating toward lower frequencies after the front hits the high-frequency end of the inertial range [10, 11].

We obtain an estimation of characteristic time for decaying wave turbulence from the kinetic equation which describes the stationary wave turbulence regime. Again, due to the finite system capacity, only a small amount of energy supply is necessary to maintain the K–Z-spectrum. In the decaying stage this supply is provided by the lowest frequencies containing most of the energy. Thus, in the decaying stage we should expect the K–Z-spectrum in the inertial range whose overall amplitude is gradually decreasing as the energy is slowly leaking from the system. Because most of the wave energy resides near the forcing frequency ω_f, the wave energy density per unit area of the water surface $\mathcal{E}$ can be estimated as E_{ω_f} as $\mathcal{E} = \int_{\omega_f} E_\omega\, d\omega \sim E_{\omega_f}\,\omega_f$. Thus, for the energy dissipation rate $\epsilon = -\dot{\mathcal{E}} \sim -\dot{E}_{\omega_f}\,\omega_f$. Substituting ϵ from the K–Z-spectrum taken at ω_f, we have

$$\dot{E}_{\omega_f} \sim -\epsilon/\omega_f \sim -E_\omega^3\, g^{-6}\omega_f^{11}. \tag{3}$$

This gives

$$E_{\omega_f} \sim \frac{g^3}{\omega_f^{11/2}}\, t^{-1/2}. \tag{4}$$

Thus according to the weak turbulence theory the peak of the energy spectrum should decay as an inverse square root of time.

Finally, let us estimate characteristic time of linear dissipation occurring at the lateral walls of the flume. Linear dissipation on the walls becomes dominant at smaller wave amplitudes. The estimate could be made based on the well-known textbook problem about the oscillating laminar flow with velocity amplitude u and frequency ω near a flat boundary. This layer has an exponential velocity profile with thickness $\delta \sim \sqrt{2\nu/\omega}$ and, therefore, the energy dissipation rate in this layer is $2\nu\delta^{-2}u^2V \sim \omega u^2 V$, where $V = 4L\delta H$ is the total volume of the boundary layer, with L being the flume size and $H \sim g/\omega^2$ being the characteristic depth of the wave motion. Dividing the energy dissipation rate in the layer by the total wave energy u^2L^2H, we get the exponent of the exponential decay of the wave energy due to the wall friction:

$$\sigma_\nu \sim \frac{4\sqrt{2\omega\nu}}{L}. \tag{5}$$

Substituting here $\nu = 10^{-6}\,\text{m}^2/\text{s}$, $\omega \sim \omega_f = 2\pi\,\text{s}^{-1}$ (1 Hz forcing) and $L \sim 10\,\text{m}$, we get $\sigma_\nu \sim 1/1000\,\text{s}^{-1}$.

In addition we can estimate the amplitude η_c corresponding to the crossover from the dominant cascade to the friction dissipation mechanism. It occurs when $\tau_K\sigma_\nu \sim 1$, which, taking into account (2), gives $\eta_c \sim 3$ cm. Thus we see that when the wave amplitudes will reach to just 3 cm we should expect that the cascade dominated dissipation of energy should be replaced by the wall friction mechanism. For the crossover time we have $t_c \sim \tau_K \ln(5/3) \sim 500\,\text{s}$. Because of the singular character of the $t^{-1/2}$ law at $t = 0$, the crossover time is almost insensitive to the initial wave intensity.

Experimental procedures. Our experimental setup was the same as described in [7]. The flume with dimensions $12 \times 6 \times 1.5\,\text{m}^3$ was filled with water up to the depth of 0.9 m. The gravity waves were excited by a piston-type wave maker consisting of 8 separate sections covering the short side of the flume. The wave

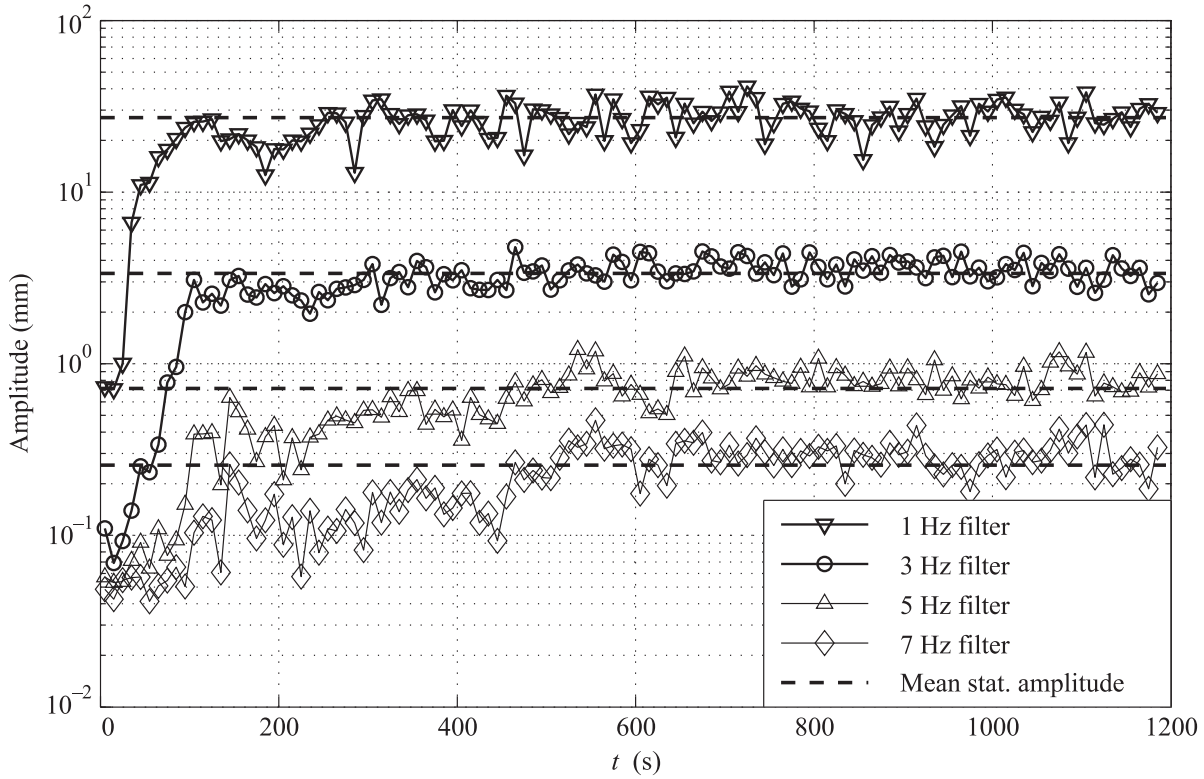

Fig. 1. The time evolution of the band passed filtered wave amplitudes in the rising wave turbulence regime for the record with $\gamma = 0.25$. Filter frequencies are equal to 1, 3, 5, 7 Hz. The bandwidth of 1 Hz is the same for all frequencies. Dashed lines show the averaged levels of filtered amplitudes in the stationary stage

maker generated a superposition of two waves of equal amplitudes and with frequencies $f_1 = 0.993$ Hz and $f_2 = 1.14$ Hz (the wavelengths are 1.58 and 1.2 m correspondingly). The wave vector k_1 was perpendicular to the plane of the wave maker and k_2 was at the angle 9° to k_1. The dissipation for one-meter waves is sufficiently low and the waves undergo multiple reflections from the flume walls, interact to each other and form a chaotic wave field homogeneous in the central area of the flume. The main control parameter was the oscillation amplitude of the wave maker.

We used two capacitance wire probes to measure the wave elevation as a function of time, $\eta(t)$. The probes were fixed at a distance 2 m from each other in the central part of the flume. Simultaneously with these point-like measurements, we recorded cross-sectional images of the air-water interface using a fluorescent technique and obtained $\eta(x,t)$, see [7] for details. Here x is a coordinate along the axis paralleled to the long side of the flume. From the wire probe data we calculated the frequency spectra at fixed x. From the images we got the one-dimensional time averaged k-spectra each calculated with using the Hamming window from 1000 points separated by 1 mm.

The whole experiment was organized as a set of records. Each record corresponds to a fixed wave maker amplitude. The record started at $t_0 = 0$ when the wave maker was switched on. The rising regime lasted up to 15 min. The wave maker was switched off at $t_f = t_0 + 40$ min after the start when the wave field became stationary. A stationarity of the wave field was estimated by observing the RMS of the wave amplitude, $\sqrt{\langle \eta^2(t) \rangle}$, measured by the wire probes. The decaying phase was recorded during an hour after the wave maker was turned off. The wire probes data were acquired continuously from $t_0 = 0$, until the end of the wave decay phase. The wave profile images were recorded with the frame rate 24 Hz as a set of movies of 124 seconds duration each. The first movie starts at t_0 and covers an initial part of the rising phase. The second movie starts at $t = t_0 + 30$ min when the wave field had reached a stationary state. The 3rd movie starts when the wave maker is turned off, at $t = t_f$, and followed by the 4th and 5th movies at $t_f + 300$ s and $t_f + 600$ s correspondingly. The set of records is ordered according to a value of the nonlinear parameter $\gamma = k_f \langle \eta \rangle$.

Experimental results. To observe the wave field non-stationarity we consider time dependencies of wave

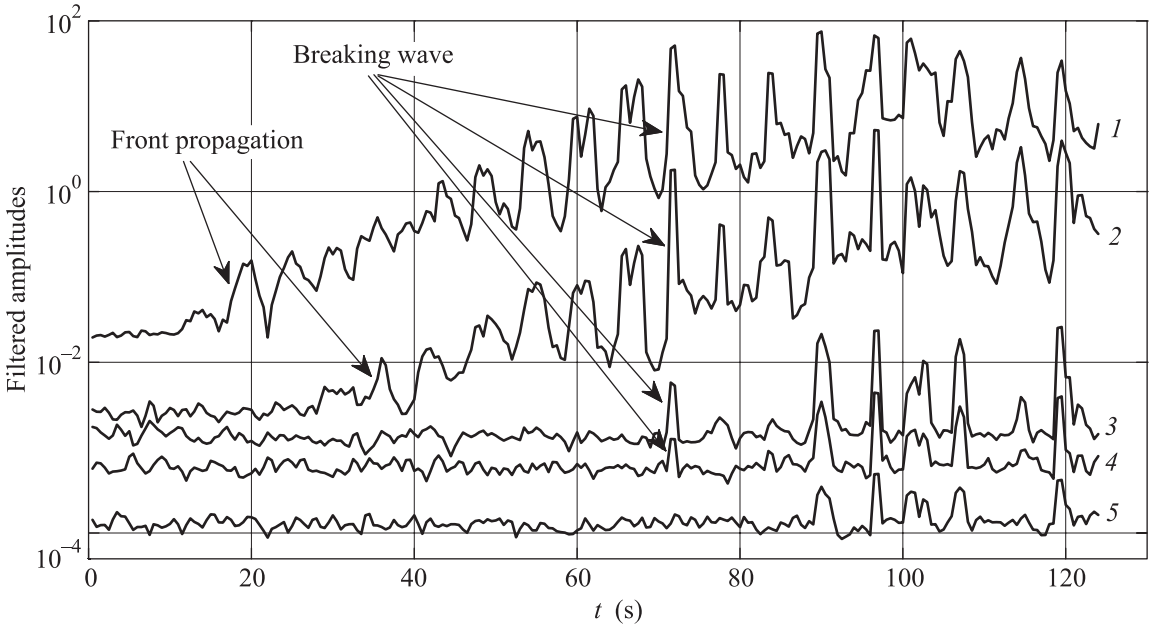

Fig. 2. Spectral amplitudes of the k-spectra as functions of time at the beginning of the wave rising phase for $\gamma = 0.35$ at the stationary phase and $1/\lambda = 2, 20, 80, 160, 320\,\mathrm{m}^{-1}$ (the plots *1*, *2*,..., *5* correspondingly)

elevations spectral amplitudes obtained by band-pass filtering in ω- and k-domains. Fig. 1 shows the rising waves in terms of time evolutions of the four spectral amplitudes, $A_i(t), i = 1, ..., 4$, filtered at frequencies $f_i = \omega_i/2\pi = 1$, 3, 5, and 7 Hz with the bandwidth 1 Hz. The wave maker was turned on at $t = 0$ with a fixed amplitude corresponding to a stationary state with $\gamma = 0.25$. The averaged stationary levels of spectral amplitudes $A_i(t)$ are shown by dash lines. As we can see, the low frequency components, 1 and 3 Hz, first reach their stationary levels in about 100 s that is fairly close to our kinetic time estimate. Higher frequency components rise with a delay and first reach their stationary levels in about 150 s, but this follows by a further adjustment time interval of about 600 s. We notice that different spectral components do not start to grow simultaneously. Instead, there is a kind of a front propagation with characteristic time of 50–100 s commensurable with the kinematic time. An additional feature in the rising phase is a relatively long adjustment interval observed for all shown components: after a fast initial increase of the spectral amplitudes up to its stationary level, they drop up to 2 times and then return back to the stationary level. The adjustment of the spectral amplitudes is slower for higher frequencies, ~ 100 s, and takes about 600 s for $f = 7$ Hz.

Fig. 2 shows k-spectral components selected from instantaneous wave profile spectra, $\eta(t_i, k)$, averaged in time over 1 s. Here the spectral energy front propagation is more evident, such that one can see 20 s delay between the wavelengths 0.5 m and 5 cm (corresponding frequencies are 1.8 and 5.6 Hz). Moreover, we can see what was happening to the short wavelength (high frequency) spectral components. They show a "fake" growth due to appearance of breaking waves whose energy synchronously spreads over a wide spectral interval and contributes to the high-frequency components in the time domain. Therefore the first time when 5 and 7 Hz components arise in Fig. 1 should be associated with the breaking events whereas the adjustment interval of 500–600 s may be considered as an actual time required for the energy to get transferred from the 1 Hz mode, corresponding to the pumping scale, down to 7 Hz, which is at the far end of the gravity wave scale. Thus we could suggest that in the beginning, before significant wave mixing has been developed, the forcing provokes breaking, probably getting in resonance with the nearest standing eigenmode of the flume.

Our previous experiments [6] showed that the slope of the stationary 1D k-spectra increases from -3.8 to -3 when the averaged wave non-linearity grows from $\gamma < 0.1$ to $\gamma \sim 0.25$. Now we can possibly identify a reason for that considering temporal fluctuations of k-spectral amplitudes in a stationary wave field shown in the upper plot of Fig. 3. The modes 2 and $20\,\mathrm{m}^{-1}$ are at the opposite sides of the gravity wave k-interval, the mode $80\,\mathrm{m}^{-1}$ is in the middle of the gravity-capillary range and $320\,\mathrm{m}^{-1}$ is in the capillary range. Large syn-

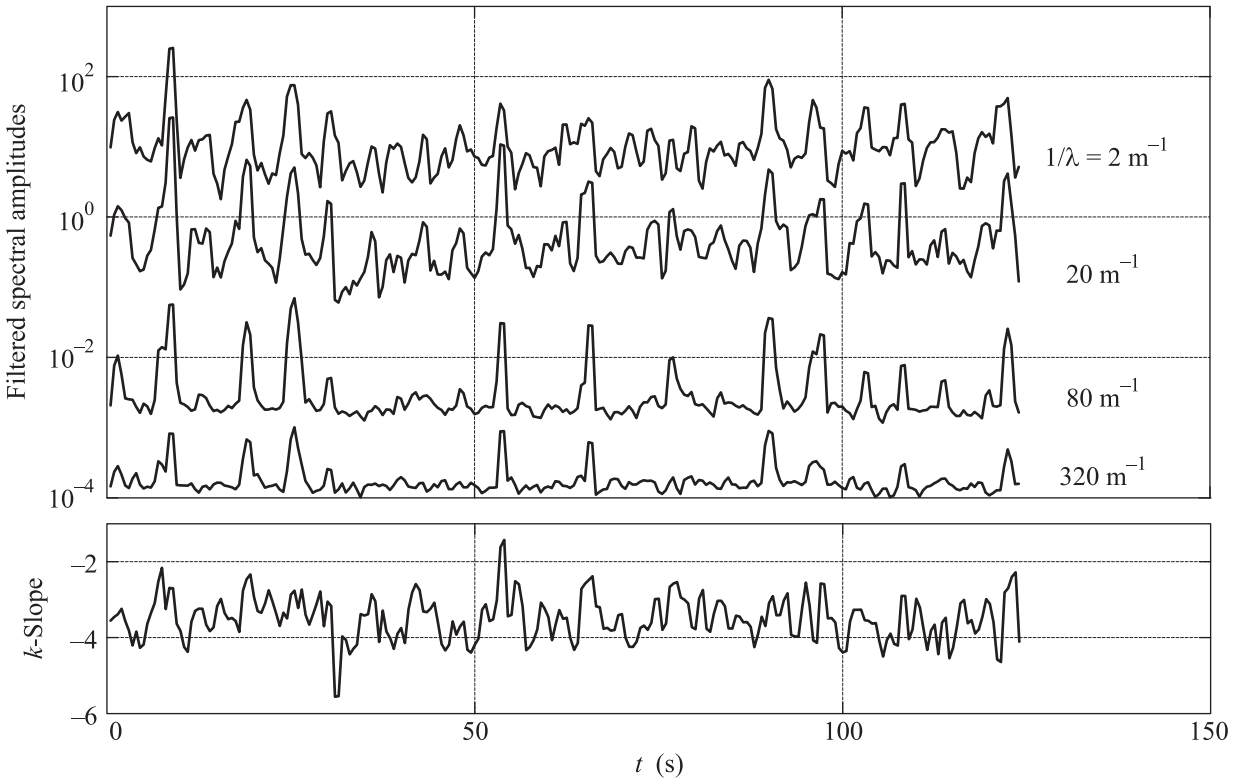

Fig. 3. Stationary regime of wave turbulence at $\gamma = 0.35$. Upper plot: time fluctuations of four wave k-modes band pass filtered at $1/\lambda = 2$, 20, 80, 320 m^{-1}. Lower plot: time dependence of the k-spectral exponents measured over the gravity range

chronous fluctuations of spectral modes are related to the wave breaking events which are characterized by a wide coherent spectrum and simultaneous peaks in amplitudes for all sampled modes. Besides these breaking events nothing significant has reached the waves at capillary range. The bottom plot in Fig. 3 shows the time fluctuations of the k-slope averaged over 1 s. There is a visible correlation between the breaking waves and increase (flattening) of the slope. Therefore, growth of the mean spectral exponent with increased forcing in our previous experiments can be explained by an increasing number of breaking events.

The decaying phase regime of wave turbulence starts when the wave maker is switched off. Fig. 4 presents the time decay of the ω-spectrum maximum at 1 Hz filtered with the 0.4 Hz bandwidth for three different experiments with $\gamma = 0.13$, 0.15, 0.18. The main plot in Fig. 4 is in the semi-logarithmic and the insert in log-log coordinates such that a difference between the power and the exponential decays is evident. For a short initial time interval the observed decay is consistent with the theoretical power law $\propto t^{-1/2}$, whereas for large time the decay is clearly exponential, with the characteristic time ~ 250 s which is faster than estimated 1000 s.

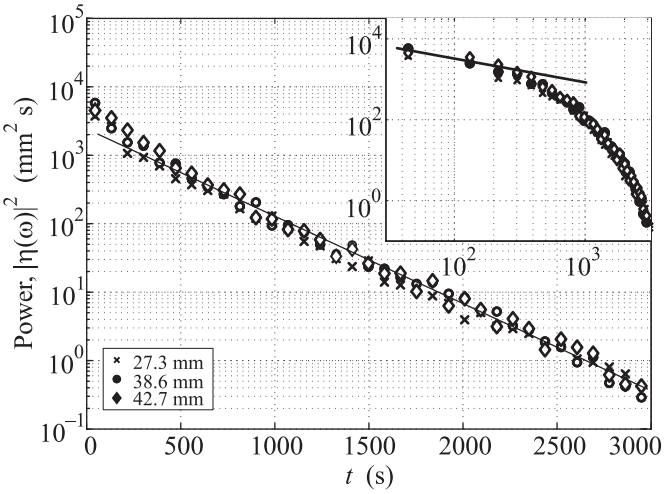

Fig. 4. Decay of the main peak of the ω-spectra of the wave elevations as a function of time for 3 initially stationary wave fields with averaged amplitudes 27.3, 38.6, and 42.7 mm ($\gamma = 0.13$, 0.15, 0.18). Measurements from the wire probe are filtered at 1±0.2 Hz (the energy containing range). Inset: the same plot in the log–log coordinates

Stronger decay could be due to additional friction at the liquid-air interface caused by an absorbed surface film. We cleaned the water surface in the flume daily

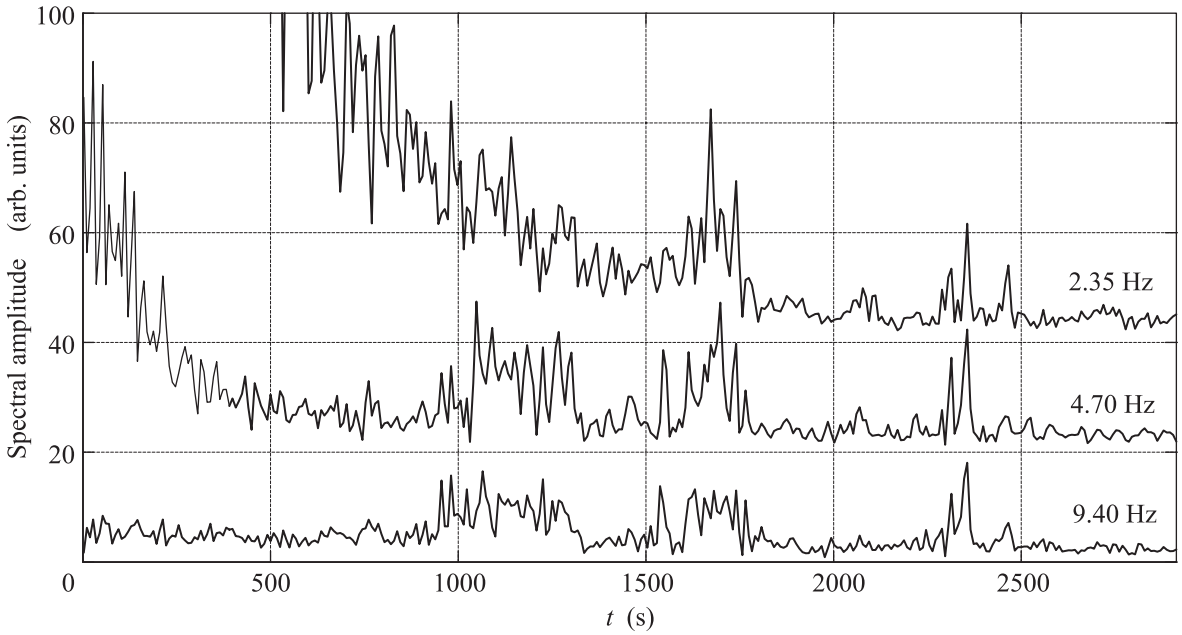

Fig. 5. Decay phase: Time evolution of the spectral amplitudes at frequencies 2.35, 4.7, and 9.4 Hz. The spectral width is 0.25 Hz. The record is with $\gamma = 0.13$ at the stationary phase. The graphs for 4.7 and 2.35 Hz are shifted vertically by 20 and 40 arb. units respectively

and checked that spectral slopes do not change during a day, but we did not check dependence of the decay exponent from surface quality. The crossover between the power law and the exponential decays occurs at about 500 s which agrees with the theoretical prediction. The crossover amplitudes and time are almost the same for different initial amplitudes. Hence, the decay curves for the three different experiments collapse onto each other on average. The exponent of the power-law cannot be determined precisely due to a comparatively short time interval of the power-law decay. The decay exponent is estimated to be somewhere between -1 and -0.5, which is consistent with the theoretical estimates.

It is interesting that despite a significant friction effect the nonlinear wave evolution remains highly nontrivial at the exponential stage of decay. To demonstrate these nontrivial nonlinear effects, we present in Fig. 5 the time evolution of three spectral modes with frequencies 2.35, 4.7, and 9.4 Hz for the experiment with the nonlinear coefficient $\gamma = 0.13$ at the stationary phase. We see that in the exponential decay region, $t > 500$ s, the spectral amplitudes decay non-monotonously. The amplitude bursts occur synchronously at different frequencies and are repeated with the characteristic time 500–700 s. A plausible explanation of such an oscillatory behaviour is that, because of the finite flume size, there exists an active cluster of discrete wave modes, consisting of one or more coupled resonant (or quasi-resonant) quartets. The cluster is semi-insulated in a sense that its wave vectors are not resonantly connected to the small-scale modes which could drain their energy via cascade and they are not too small to be strongly dissipated by the friction. Such an insulated low-dimensional system could experience quasi-periodic behaviour in a way an isolated integrable wave quartet would. It is important to reiterate that these non-trivial nonlinear oscillations are not significant for the decay of the total energy: they are not visible on the decay of the main energy peak shown in Fig. 4.

Conclusions. We considered evolving wave turbulence in its rising and decay stages. In the rising stage, we see a front in the k-space propagating toward higher k's at a timescale consistent with the kinetic equation. On the background of this slow rise we see synchronous peaks appearing across a broad range of wavenumbers which might be interpreted as breaking waves. Similar peaks observed in the steady state might be responsible for flattening of the wave spectra observed in previous experiments [6, 4].

The decaying stage displays two different types of behavior. An early decay stage proceeds in agreement with the WTT predictions: the energy decays as $t^{-1/2}$. This is followed by a longer time interval exponential decay of the wave energy, which is consistent with our estimate of the decay rate caused by the wall friction. Despite the monotonous decay of the total energy, at this stage we observe quasi-periodic synchronous oscillations of energy across the high-frequency tail of the

spectrum. We attribute these oscillations to existence of a low-dimensional cluster of resonant waves.

The authors are grateful to Dr. S. McLelland and B. Murphy for their help with the experiments at the Deep flume.

1. V. E. Zakharov, V. S. L'vov, and G. Falkovich, *Kolmogorov Spectra of Turbulence I*, Springer-Verlag, Berlin, 1992.
2. A. I. Dyachenko, A. O. Korotkevich, and V. E. Zakharov, Phys. Rev. Lett. **12**, 13 (2004).
3. P. A. Hwang and D. W. Wang, J. Phys. Ocean. **30**, 2787 (2000).
4. E. Falcon, C. Laroche, and S. Fauve, Phys. Rev. Lett. **98**, 094503 (2007).
5. P. Denissenko, S. Lukaschuk, and S. Nazarenko, Phys. Rev. Lett. **99**, 014501 (2007).
6. S. Lukaschuk, S. Nazarenko, S. McLelland, and P. Denissenko, Phys. Rev. Lett. **103**, 044501 (2009).
7. S. Nazarenko, S. Lukaschuk, S. McLelland, and P. Denissenko, Journ. of Fluid Mech. **642**, 395 (2010).
8. L. Deike, M. Berhanu, and E. Falcon, Phys. Rev. E **85**, 066311 (2012).
9. L. V. Abdurakhimov, M. Yu. Brazhnikov, and A. A. Levchenko, JETP Lett. **89**, 120 (2009).
10. G. E. Falkovich and A. V. Shafarenko, Journ. Nonlinear Sci. **1**, 457 (1991).
11. S. V. Nazarenko, *Wave Turbulence*, Springer, 2011.